

²Jankovic, M. S., "Exact n th Derivatives of Eigenvalues and Eigenvectors," *Journal of Guidance, Control, and Dynamics*, Vol. 17, No. 1, 1994, pp. 136–144.

³Jankovic, M. S., "Comments on 'Eigenvalue Sensitivity in the Stability Analysis of Beck's Column with a Concentrated Mass at the Free End'," *Journal of Sound and Vibration*, Vol. 167, No. 3, 1993, pp. 557–559.

Reply by the Author to M. S. Jankovic

Mehmet A. Akgün*
Middle East Technical University,
Ankara 06531, Turkey

JANKOVIC¹ states that the left eigenvectors of the example nonself-adjoint system are in error. Strictly speaking, they are not in error. In other words, they are valid eigenvectors. However,

is observed that $\{y_j\}^T \{x_i\}$ is of the order of 10^{-14} for $i \neq j$. $[D_E]$ is unchanged with the new choice of $\{y_2\}$. Again $\lambda_{3,g} = 10/78$, and the exact derivative of the third right eigenvector, computed with $n = -1$ with the full set of eigenvectors, i.e., with $\hat{N} = N$, comes out to be

$$\{x_3\}_{,g} = \begin{bmatrix} -2.252150672346110e-01 \\ -3.960995573373423e-01 \\ -6.410256410256399e-02 \\ 1.318383028480748e-01 \\ 2.108911718032278e-03 \\ -1.339472145661070e-01 \end{bmatrix}$$

which agrees with Jankovic's solution to the full machine precision.

The same derivative is now computed with higher order methods by using the first four modes as in the original paper.² The columns of the matrix given next show, from left to right, the derivative computed with $n = 0-7$, respectively.

$n = 0$	1	2	3	4	5	6	7
-0.2526	-0.2308	-0.2126	-0.2348	-0.2201	-0.2270	-0.2250	-0.2249
-0.3845	-0.3467	-0.4432	-0.3679	-0.4081	-0.3933	-0.3953	-0.3976
0.0794	-0.1102	-0.0630	-0.0523	-0.0749	-0.0578	-0.0667	-0.0635
0.0363	0.1246	0.1648	0.1046	0.1469	0.1260	0.1328	0.1326
0.0170	0.0333	-0.0298	0.0218	-0.0065	0.0043	0.0025	0.0011
-0.0533	-0.1579	-0.1350	-0.1263	-0.1404	-0.1303	-0.1354	-0.1337

$\{y_2\}$ is not biorthogonal to $\{x_1\}$. This is a good example of a case where special care is required in assuring that the eigenvectors corresponding to a multiple eigenvalue are (bi)orthogonal. The wrong choice of the second left eigenvector was an oversight by the author and the author thanks Jankovic for noticing the error in the computed eigenvector derivative. In Ref. 2, $\{y_2\}$ not being biorthogonal to $\{x_1\}$ led to a wrong value for a_{jk2} , Eq. (16). The exact value of the derivative of the third right eigenvector at the bottom of page 384 was computed with $n = -1$, i.e., the so-called modal method, with the full set of eigenvectors. Since, both the exact value and the values for various n with a truncated set of eigenvectors (top of page 385) used the same incorrect value of a_{jk2} , the latter converged to the former, which was itself in error, and as a result, the mistake went unnoticed. This mistake, however, does not in any way affect the conclusions about the performance of the family of modal methods developed in the paper as will be illustrated next. The matrix $[A]$ and the matrix of right eigenvectors $[X]$ will not be repeated here and can be looked up in the paper or in Jankovic's Comment.¹ The $\{y_j\}$ for $j \neq 2$ need not be repeated either. The newly selected $\{y_2\}$ is

$$\{y_2\}^T = [-0.5 \quad 2 \quad 6.8 \quad 18.4 \quad 15.9 \quad 6.3]$$

In the paper,² most of the eigenvectors were computed with Eispack routines. They are computed again here with Matlab this time as was done by Jankovic. Their biorthogonality is checked, and it

The derivative values computed with $n = 12$ and 20 are, on the other hand,

$n = 12$	$n = 20$
-2.2521e-01	-2.252153e-01
-3.9614e-01	-3.960991e-01
-6.4060e-02	-6.410227e-02
1.3184e-01	1.318378e-01
2.0840e-03	2.109269e-03
-1.3392e-01	-1.339470e-01

where the number of significant digits used are different to point out the convergence to the exact value. In practice, the 20th-order method would never be used. But then, the example problem, which is of size 6, would be solved with $n = -1$ by using the full set of eigenvectors because 1) the magnitude of the third eigenvalue not being very small compared to the modulus of the fifth and sixth eigenvalues requires a high-order method (i.e., a large value of n) for convergence when the fifth and sixth eigenvectors are not used, and 2) the computational saving, if any, with the use of a high-order method is insignificant for such a small system. The example was intended to demonstrate the convergence of the method for a system with a qualitative relative moduli trend of eigenvalues as described. For large practical systems, however, where the eigenvalues associated with the eigenvector derivatives of interest are much smaller in magnitude than most of the system eigenvalues, a low-order method with a small subset of the eigenvectors is sufficient for convergence. And 14 digit accuracy is hardly required in practical engineering analysis. Jankovic is to be commended for his exact solution of eigenvector derivatives. His assertion¹ that "the existence of exact analytical solutions obviates the need for using any numerical method," however, should be taken with some reser-

Received May 6, 1994; accepted for publication June 7, 1994. Copyright © 1994 by the American Institute of Aeronautics and Astronautics, Inc. All rights reserved.

*Associate Professor, Aeronautical Engineering Department. Member AIAA.

vation in cases where number of flops is an issue and for reasons just described.

The flop count for Jankovic's method when computing the first derivatives of p right eigenvectors with respect to q design parameters is given next for $[B] = [I]$.

- 1) Compute the first p left and right eigenvectors (same count as for EISPACK subroutines). : $3.5pN^2$
- 2) Compute $\{x_j\}\{x_j\}^T$ for $j = 1, \dots, p$. : pN^2
- 3) LU decompose $[Q]^{-1} \equiv ([A] - \lambda_j[I] + \{x_j\}\{x_j\}^T)$.
for $j = 1, \dots, p$. : $pN^3/3$
- 4) For $j = 1, \dots, p$ and $k = 1, \dots, q$:
a) Compute $[A]_{,k}\{x_j\}$ where : $pqN^2\kappa$
 κ is a sparsity parameter which is unity for full $[A]_{,k}$.
b) Compute $[Q]([A]_{,k}\{x_j\})$. : pqN^2

The total number of flops is thus $[4.5p + pN/3 + pq(\kappa + 1)]N^2$. The flop count for computing the eigenvalues is not considered since the same count will appear in both methods to be compared. The flop count for the n th-order modal method is, on the other hand,

$$[3.5\hat{N} + N/3 + pq(\kappa + 1 + n)]N^2$$

The flop count for the n th-order modal method is thus smaller than that for Jankovic's method when

$$nq/N < z - 1/3p; \quad z \equiv 1/3 + (4.5 - 3.5e)/N, \quad e \equiv \hat{N}/p$$

As explained in the paper² (p. 386), a good value for e may be 3.0 for $N = 100$ which gives $z = 0.27$ and z increases for larger system sizes which makes the n th-order method more advantageous. For the first-order method, i.e., for $n = 1$, Jankovic's method is advantageous when only a single derivative is of interest, i.e., for $p = 1$. For larger number of eigenvector derivatives, the first-order method is preferable when the number of design parameters to be varied is not unusually high. On the other hand, the method $n = -1$ with the full set of eigenvectors used outperforms Jankovic's method when p is greater than about 10 or 11.

References

- ¹Jankovic, M. S., "Comment on New Family of Modal Methods for Calculating Eigenvector Derivatives," *AIAA Journal*, Vol. 33, No. 5, 1995, pp. 965-967.
- ²Akgin, M. A., "New Family of Modal Methods for Calculating Eigenvector Derivatives," *AIAA Journal*, Vol. 32, No. 2, 1994, pp. 379-386.

Comment on "Induced Drag of Wings of Finite Aspect Ratio"

A. W. Bloy* and M. Jouma'a†
University of Manchester,

Manchester M13 9PL, England, United Kingdom

IN Ref. 1 Lam modifies lifting-line theory using an approximate model of wing wake roll up to determine the effect of roll up on induced drag. Elliptic wing loading is considered, and the wake model consists of a flat trailing vortex sheet of finite length. This vortex sheet is assumed to roll up suddenly at some distance ℓ downstream to form two discrete trailing vortices which, for elliptic loading, are spaced a distance of $\pi/4$ times the wing span apart. However this

Received Sept. 27, 1993; accepted for publication June 3, 1994. Copyright © 1994 by the American Institute of Aeronautics and Astronautics, Inc. All rights reserved.

*Lecturer, Department of Engineering.

†Research Student, Department of Engineering.

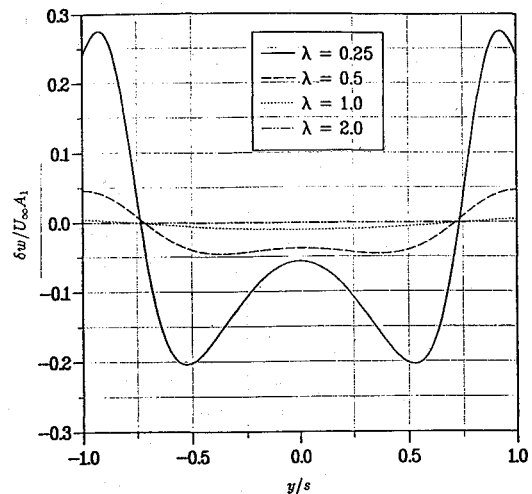


Fig. 1 Induced downwash over the wing due to crossflow vortices.

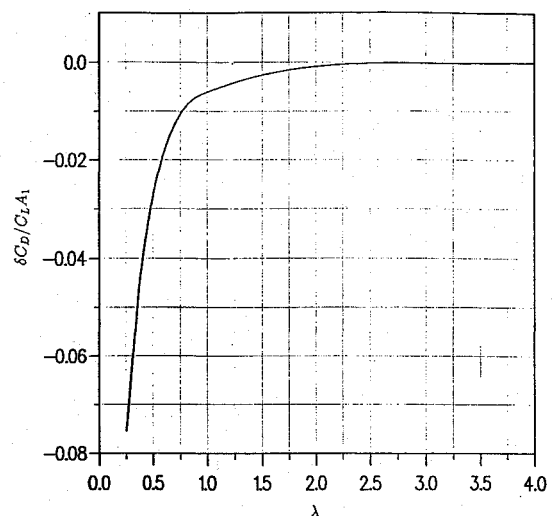


Fig. 2 Induced drag increment due to crossflow vortices.

roll-up model allows the vortex lines which trail in the freestream direction to end in the fluid at the downstream position at which the sudden roll up occurs.

A roll-up model using continuous vortex lines is considered here. At the roll-up position the vortices from the trailing vortex sheet are assumed to turn across the flow and merge into the two discrete trailing vortices. There are then three contributions to the induced downwash on the wing. The two contributions from the vortex sheet and the discrete trailing vortices are analyzed by Lam¹ and the remaining contribution, analyzed here, is that due to the trailing vortices in the crossflow direction. Inboard of the two discrete trailing vortices the crossflow vortices are in the same direction as the wing bound vortex whereas outboard the opposite applies. The inboard crossflow vortices, therefore, produce upwash over the wing whereas the outboard vortices produce downwash. From the Biot-Savart law the induced downwash velocity increment δw at a spanwise position y' on the wing is given by

$$\delta w = -\frac{1}{4\pi} \int_{-s}^s \frac{G\ell}{[(y-y')^2 + \ell^2]^{3/2}} dy \quad (1)$$

where $G(y)$ denotes the spanwise circulation distribution of the crossflow vortices. In Eq. (1) s is the wing semispan. In terms of the wing spanwise circulation distribution $\Gamma(y)$, $G(y) = -\Gamma(y)$ outboard of the two discrete trailing vortices and inboard $G(y) = \Gamma_{y=0} - \Gamma(y)$.

The downwash distributions have been calculated at the values of $\lambda (= \ell/s)$ used by Lam¹ and are shown in Fig. 1 where the down-